*Supporting Information for*

# Orthogonally Activatable CRISPR-Cas13d Nanoprodrug to Reverse Chemoresistance for Enhanced Chemo-Photodynamic Therapy

Zheng Liu,[a] Zhiyuan Feng,[a] Mohan Chen,[a] Jiayin Zhan,[a] Rong Wu,[a] Yang Shi,[a] Yunsheng Xue,[b] Ran Liu,[a] Jun-Jie Zhu,[a] and Jingjing Zhang*[a]

[a]State Key Laboratory of Analytical Chemistry for Life Science, School of Chemistry and Chemical Engineering, Chemistry and Biomedicine Innovation Center (ChemBIC), Nanjing University, Nanjing 210023, China. E-mail: jing15209791@nju.edu.cn.

[b]Jiangsu Key Laboratory of New Drug Research and Clinical Pharmacy, School of Pharmacy, Xuzhou Medical University, Xuzhou 221004, China.

## Contents

## Experimental Procedures

### Chemicals and Materials

Neodymium (III) chloride hexahydrate ($NdCl_3 \cdot 6H_2O$, 99.9%), yttrium (III) chloride hexahydrate ($YCl_3 \cdot 6H_2O$, 99.9%), ytterbium (III) chloride hexahydrate ($YbCl_3 \cdot 6H_2O$, 99.9%), thulium (III) chloride hexahydrate ($TmCl_3 \cdot 6H_2O$, 99.9%), Holmium (III) chloride hexahydrate ($HoCl_3 \cdot 6H_2O$, 99.9%), tetraethyl orthosilicate (TEOS, 99%), DSPE-$PEG_{2000}$, 1,2-dioleoyl-sn-glycero-3-phosphoethanolamine (DOPE, 98%), cholesterol (95%), (3-aminopropyl)triethoxysilane (APTES, 98%), ammonium fluoride ($NH_4F$, 98%), and sodium hydroxide (NaOH, 99.9%) were purchased from Aladdin Co., Ltd. Petroleum ether (PE, AR), ethyl acetate (EA, AR), ethyl ether, and methanol (MeOH, AR) were obtained from Sinopharm Chemical Reagent Co., Ltd. Oxaliplatin (99%), and glutathione (GSH) were acquired from Beijing Hwrk Chemical Co., Ltd. 6-Bromohexanoic acid (97%), and Rose Bengal (RB, 95%) were purchased from Sigma-Aldrich Chemical Reagent Co., Ltd. 4% paraformaldehyde fix solution, and RPMI-1640 were purchased from Jiangsu KeyGEN BioTECH Corp., Ltd. Fetal bovine serum was obtained from ZhejiangTianhang Biotechnology Co.Ltd. Protease inhibitor cocktail and 1,2-Dioleoyl-3-trimethylammonium-propane chloride (DOTAP) were acquired from TargetMol Chemicals Inc. Serum-free cell freezing medium (CELLSAVING) was purchased from New Cell & Molecular Biotech Co.,Ltd. The DNA (see Table S1) were synthesized from Sangon Biotech Co., Ltd. (Shanghai, China). The ultrapure water used in all experiments was Millipore water (18.2 MΩ).

### Characterization

Transmission electron microscopy (TEM) images were recorded on a FEI Tecnai G20 microscope at 200 kV. The hydrodynamic size and ζ-potentials of samples were measured by Zetasizer Nano series Nano-ZS (Malvern Instrument Ltd, UK). UV-vis absorption spectra were recorded using an UV-8000 spectrophotometer (Shanghai Metash Instrument Co., Ltd., China). Cell viability data were obtained using a Biotek Synergy H1 microplate reader (BioTek, USA). The photoluminescence spectra were collected by using FLS980 spectrometer (Edinburgh Instruments, UK), and F320 spectrometer (Tianjin Gangdong Sci.&Tech. Co., Ltd., China). $^{1}H$ and $^{13}C$ nuclear magnetic resonance (NMR) spectra of samples were recorded on a Bruker Avance III 400 spectrometer. The *in vivo* fluorescence images were obtained from a IVIS Lumina XRMS Series III (PerkinElmer, USA).

### Synthesis of RB-HA

Rose Bengal-hexanoic acid (RB-HA) was prepared through the conventional method with slight modifications.[1-3] Briefly, RB sodium salt (1.0 g; 1.03 mmol) and 6-bromohexanoic acid (0.6 g; 3.1 mmol) were dissolved in 10 mL of N, N-Dimethylformamide (DMF), then the mixture was heated to 80 °C and maintained for 6 h. After the solution of DMF was distilled off in vacuo, the product was stirred with 50 mL of diethyl ether overnight and collected by centrifugation. In order to remove excess RB sodium salt, 50 mL of deionized water was added. Finally, RB-HA was collected by centrifugation and purified by silica gel column chromatography to afford a purple powder. Yield: 0.84 mmol (82%).

### Synthesis of RB-NHS

To activate the carboxyl group of RB-HA, RB-HA (500 mg; 0.46 mmol), 4 equivalent of N-hydroxysuccinimide (NHS), and 3 equivalent of 1-ethyl-3-(dimethylaminopropyl) carbodiimide (EDC) were dissolved in 8 mL of DMF and the mixture was stirred overnight at RT. When the solution of DMF was distilled off in vacuo, the product was washed with excess water and chloroform. After the product was enriched in 5 mL of chloroform, 50 mL of diethyl ether was added to precipitate the product. Finally, RB-NHS was collected by centrifugation and purified by silica gel column chromatography to afford a deep purple powder. Yield: 0.35 mmol (76%).

**Synthesis of RB-Pt**

After RB-NHS (100 mg; 0.08 mmol) and [Pt (DACH)$(OH)_2$(ox)] (50 mg; 0.1 mmol) were added to 5 mL of dimethyl sulfoxide (DMSO), the solution was stirred at 60 °C overnight at RT. After the solution was added to chloroform (20 mL) dropwise, the product was collected by centrifugation and purified by running a prep TLC (Preparative Thin Layer Chromatography). Yield: 0.04 mmol (50%).$^1$H NMR (400 MHz, DMSO-d6 ): δ 8.60 (s, 1H), 8.20 (s, 1H), 7.79 (s, 1H), 7.47 (s, 1H), 3.88 (t, J = 10 Hz, 2H), 2.50 (m, 2H), 2.01 (t, J = 10 Hz, 2H), 1.52 – 1.41 (m, 4H), 1.17 – 1.14 (m, 4H), 0.94 – 0.80 (m, 6H), $^{13}$C NMR (DMSO-$d_6$ ): δ 182.4, 172.3, 164.5, 163.7, 162.8, 157.5, 139.3, 136.6, 135.4, 134.8, 134.2, 132.3, 130.4, 130.1, 129.3, 110.7, 97.8, 76.4, 66.6, 60.6, 36.3, 31.3, 29.5, 28.1, 27.0, 25.5, 25.3, 24.2. ESI-HRMS (positive ion mode) m/z: $[M + Na]^+$ calculated for $C_{34}H_{28}Cl_4I_4N_2O_{12}Pt$ 1501.10; found 1524.6125.

**Computational Methods**

Density functional theory (DFT) and time-dependent DFT(TD-DFT) calculations were performed using the Gaussian 09 program package.

**Construction, expression, and purification of Cas13d protein**

The coding sequence of Cas13d was derived from the plasmid pET28a-MH6-RspCas13d (Addgene, #108305). For protein expression of Cas13d, the plasmid was transformed to *Escherichia coli* Rosetta (DE3) Competent Cells, and a single *E. coli* colony was picked and inoculated into 5 mL of liquid Luria-Bertani (LB) tubes containing 50 μg/ml Kanamycin at 37 °C overnight. Then, the liquid was transferred into 1 L of fresh LB medium (Kanamycin: 50 μg/mL) and inoculated in a shaking incubator until optical density (OD) at 600 nm ($OD_{600}$) reached 0.6 at 37 °C. Cas13d was expressed by inducing the *E.coli* cells with 0.2 mM isopropyl-1-thio-D-galactopyranoside (IPTG) for 18 h at 16 °C. Then cells were harvested by centrifugation (8,000 rpm, 10 min, 4 °C), and resuspended in lysis buffer (20 mM Tris-HCl, 10 mM imidazole, 500 mM NaCl, pH = 7.5) containing 0.2 mg/ml lysozyme and 1 mM phenylmethylsulfonyl fluorid (PMSF). After sonication, the supernatant was collected, passed through a membrane filter (pore size 0.45 μm) and incubated with Ni-NTA Affinity Column for 1 h. The protein binding buffer (20 mM Tris-HCl, 500 mM NaCl, 20 mM imidazole, pH = 7.5) and protein elution buffer (20 mM Tris-HCl, 500 mM NaCl, 250 mM imidazole, pH = 7.5) were used to harvest protein Cas13d. Finally, the protein was concentrated by a 30 kDa MW cut off filter and stored in storage buffer (20 mM Tris-HCl, 300 mM NaCl, 50% glycerol,1 mM DTT, pH = 7.5) at -20 °C for further use.

**Design and preparation of sgRNAs**

The sgRNAs for the ABCC1 (MRP1) gene were designed using the online software (https://cas13design.nygenome.org). Target sites for the sgRNAs were designed by seeking appropriate sequences in the ABCC1 mRNA (Gene Bank: NM-0049996.4). To check off-target effects of the sgRNAs, basic local alignment search tool (BLAST) was then used to check off-target effects of the sgRNAs and the specificity of the target gene. For the synthesis of sgRNAs, the constructs were sequenced to DNA with additional T7 promoter sequences. After the sgRNAs were annealed into short T7 primers, T7 polymerase was added and incubated overnight at 37 °C using HyperScribe™ T7 High Yield RNA Synthesis Kit. Finally, the sgRNA was purified using Monarch RNA Cleanup Kit (500 μg) according to the manufacturer's instructions. The oligonucleotides are listed in **Table S1**.

**Synthesis of $NaYF_4$:20%Nd/20%Yb@$NaYF_4$:30%Yb/0.5%Tm@$NaYF_4$@$NaYbF_4$:1%Ho@$NaYF_4$ upconversion nanoparticles (UCNPs)**

**Step 1: Synthesis of β-$NaYF_4$:20%Nd/20%Yb core UCNPs**

The core UCNPs were prepared through the conventional method.[4,5] In a typical experiment, $YCl_3 \cdot 6H_2O$ (0.6 mmol), $YbCl_3 \cdot 6H_2O$ (0.2 mmol) and $NdCl_3 \cdot 6H_2O$ (0.2 mmol) were added into a flask containing oleic acid (6 mL) and 1-octadecene (10 mL) to prepare precursor at 150 °C for 60 min under the protection of nitrogen. Then, the clear solution was cooled down to room temperature (RT) followed by addition of 10 mL of methanol solution containing $NH_4F$ (150 mg; 4 mmol) and NaOH (100 mg; 2.5 mmol). The slurry was heated to 80 °C and maintained for 1 h with vigorous stirring under the protection of nitrogen. Finally, the mixture was heated to 300 °C at a rate of ≈ 15 °C/min and maintained for 60 min with nitrogen protection. After the solution was cooled down to RT, β-$NaYF_4$:20%Nd/20%Yb core UCNPs were precipitated from the mixture by addition of an excess of ethanol, centrifuged (10,000 rpm, 10 min), and re-dispersed in 5 mL of cyclohexane for further shell growth.

**Step 2: Synthesis of core-multishell structured UCNPs**

The core-multishell UCNPs ($NaYF_4$:20%Nd/20%Yb@$NaYF_4$:30%Yb/0.5%Tm@$NaYF_4$@$NaYbF_4$:1%Ho@ $NaYF_4$) were synthesized by using β-$NaYF_4$:20%Nd/20%Yb as cores for subsequently shell coating. Take $NaYF_4$:20%Nd/20%Yb@$NaYF_4$:30%Yb/0.5%Tm for example, $YCl_3 \cdot 6H_2O$ (0.695 mmol), $YbCl_3 \cdot 6H_2O$ (0.3 mmol) and $TmCl_3 \cdot 6H_2O$ (0.005 mmol) were added into a 100-mL three-necked flask containing oleic acid (6 mL) and 1-octadecene (10 mL), the mixture of solvents was heated to 150 °C and maintained 60 min under the protection of nitrogen. After the solution was cooled down to RT, 10 mL of methanol solution containing $NH_4F$ (150 mg; 4 mmol), NaOH (100 mg; 2.5 mmol) and 5 mL of cyclohexane containing 1 mmol core UCNPs were added, then the slurry was heated to 80 °C and maintained for 1 h with vigorous stirring under the protection of nitrogen. Finally, the mixture was heated to 300 °C at a rate of 15 °C/min and maintained for 60 min. The as-prepared $NaYF_4$:20%Nd/20%Yb@$NaYF_4$:30%Yb/0.5%Tm core-shell (CS) UCNPs were precipitated from the mixture by addition of an excess of ethanol, centrifuged, and re-dispersed in 5 mL of cyclohexane for further shell growth. The precursors of shell (1 mmol $YbCl_3 \cdot 6H_2O$, 4 mmol $NH_4F$, and 2.5 mmol NaOH)

were used for the synthesis of $NaYF_4$:20%Nd/20%Yb@$NaYF_4$:30%Yb/0.5%Tm@$NaYF_4$ core-shell-shell (CSS) UCNPs. The precursors of shell (0.99 mmol $YbCl_3 \cdot 6H_2O$, 0.01 mmol $HoCl_3 \cdot 6H_2O$, 4 mmol $NH_4F$, and 2.5 mmol NaOH) were used for the synthesis of $NaYF_4$:20%Nd/20%Yb@$NaYF_4$:30%Yb/0.5%Tm@$NaYF_4$@$NaYbF_4$:1%Ho core-shell-shell-shell (CSSS) UCNPs. Finally, the precursors of shell (1 mmol $YCl_3 \cdot 6H_2O$, 4 mmol $NH_4F$, and 2.5 mmol NaOH) were used for the preparation of $NaYF_4$:20%Nd/20%Yb@$NaYF_4$:30%Yb/0.5%Tm@$NaYF_4$@$NaYbF_4$:1%Ho@$NaYF_4$ core-shell-shell-shell-shell (CSSSS) UCNPs.

**Synthesis of UCNP/Silica core-shell sructures**

In a typical procedure, the core-multishell structured UCNPs (0.2 mmol) in cyclohexane (200 μL) were poured into cetyltriethyl-ammnonium bromide (CTAB) aqueous solution (5 mg/mL), and the solution was stirred overnight to generate a transparent UCNP@CTAB solution. After 6 mL of ethanol, 10 mL of deionized water, and 100 μL of NaOH solution (2 M) were added to the reaction solution, the solution was heated to 70 °C under vigorously stirring. After 50 μL of tetraethyl orthosilicate (TEOS) was slowly added to the solution within 10 min, the mixture was stirred for 10 min another. The as-synthesized UCNP@$SiO_2$ NPs were collected by centrifugation and washed with ethanol twice to remove the excess CTAB. Then, 220 μL of HCl was added to ethanol (50 mL) containing UCNP@$SiO_2$ NPs, and the resultant solution was heated to 60 °C and stirred for 3 h. The as-synthesized UCNP@m$SiO_2$ NPs were collected by centrifugation and washed with ethanol to remove the excess HCl. After UCNP@m$SiO_2$ NPs were re-dispersed into 50 mL of ethanol solution, 1-mL ethanol containing 40 μL of triethoxy-3-aminopropylsilane (APTES) was added and the solution was heated to 70 °C for 3 h. Finally, amino modified UCNP@m$SiO_2$ NPs were collected by centrifugation and washed twice with ethanol.

**Preparation of UCNP@RB-Pt**

Firstly, UCNP@m$SiO_2$ (10 mg), and RB-Pt (1 mg) were dissolved in 2 mL of DMF solution, and the mixture was magnetically stirred at RT for 12 h. Secondly, the RB-Pt loaded NPs were collected via centrifugation at 11,000 g for 10 min. To remove the excess RB-Pt, the UCNP@RB-Pt NPs were washed with DMF and then dispersed in deionized water for further use. Finally, the loading amount of RB-Pt was determined by the UV absorption at wavelength of 575 nm.

**Irradiation of protectors and their characterization by HPLC and XPS analysis**

To determine the product of photo-controlled release of the RB-Pt prodrug, 2.5 μg of UCNP@RB-Pt NPs were added into 50 μL of PBS at pH 7.4 with or without 10 mM GSH, then the solution was irradiated with or without 980 nm laser (0.5 W/$cm^2$, 5 min). After incubated for 24 h, the mixture was added into 50 μL of DMF and centrifuged at high speed to collect the red supernatant. After filtration with a 0.22 μm membrane, the solution was diluted 4 times with water and then analyzed by HPLC. Briefly, a 250 × 4.6 mm $C_{18}$ column (ShimNex HE, C18-AQ) was used with mobile phase containing water (A) and acetonitrile with 0.1% formic acid (B). 40 μL of sample was injected in the HPLC and samples were ran using a gradient: 95% A to 95% B over 20 min. To determine the valence state of the resulting product,

the 20 mg of UCNP@RB-Pt NPs was dissolved in PBS buffer containing 10 mM GSH, then the solution was irradiated with or without 980 nm light (0.5 W/cm$^2$, 15 min). After incubated for 24 h in the dark, the solution was lyophilized and collected for XPS analysis.

**Preparation of RNP**

The sgRNA and PC-linker-modified ssDNA were purchased from Sangon Biotech and reconstituted in RNase free water (10 μM), then the PC protector DNAs and sgRNA were then added into 40 μL of buffer (20 mM Tris-HCl, 100 mM NaCl, 5 mM $Mg^{2+}$, pH = 7.9) at a 1.1:1 volume ratio to the sgRNA/PC-DNA complex, and the mixture was heated to 95 °C in a heat block for 5 min and then the heat block was turned off to allow slow cooling of the mixture to room temperature. To form RNP complexes, Cas13d protein was then incubated with sgRNA/PC-DNA complex at a 2:1 molar ratio in 80 μL of buffer (20 mM Tris-HCl, 100 mM NaCl, 5 mM $Mg^{2+}$, pH = 7.9) at 37 °C for 15 min.

**Preparation of UCNP@RB-Pt/RNP**

For RNP loading, the UCNP@RB-Pt and RNP were added into RNase free water at the molar ratio of RNP to UCNP@RB-Pt NPs was 1 to 200. Then this mixture was incubated in the dark at 4 °C for 15 min with shaking. Then UCNP@RB-Pt/RNP NPs were collected by centrifugation (10,000 rpm, 5 min) and resuspended in deionized water for further use.

**Synthesis of liposome**

To synthesize liposome modified with cRGD, DOTAP (2 mg, 2.9 μmol), cholesterol (0.5 mg,1.3 μmol), DOPE (0.1mg, 0.17 μmol), DSPE-$PEG_{2000}$ (0.028 mg, 0.014 μmol) were mixed in a vial containing 50 μL of chloroform. After the chloroform evaporated naturally in a fume hood, the vial was heated to 100 °C and maintained at 100 °C for 2 min, then the mixed solution of ethanol/sodium acetate buffer (1 mL, v/v ratio = 9: 1, pH = 5.2) was added dropwise to the vial to hydrate the lipid film. Then DSPE-$PEG_{2000}$-cRGD (0.036 mg, 0.014 μmol) was added to above solution to form cRGD modified liposome. Finally, after the mixture was incubated at 37 °C for 30 min, ultrafiltration centrifugal tube (1,000 kDa cut-off) was used to purify this above liposome. To synthesize cRGD-free liposome, synthesis method was consistent with the cRGD modified liposome only with slight modification. After hydration of the phospholipid layer, 0.014 μmol of DSPE-$PEG_{2000}$-cRGD was replaced by DSPE-$PEG_{2000}$ (0.014 μmol), and then the mixture was incubated and purified.

**Preparation of UCNP@RB-Pt/RNP@liposome and cRGD-free UCNP@RB-Pt/RNP@liposome**

To coat the UCNP@RB-Pt/RNP NPs with liposome, 400 μL of 0.5 mg/mL liposome was added to 100 μL of 2 mg/mL UCNP@RB-Pt/RNP. After vortexed for several seconds, the mixture was incubated at 4 °C with shaking for 30 min. Afterwards, the UCNP@RB-Pt/RNP@liposome NPs were collected by centrifugation (11,000 rpm, 10 min) and resuspended in deionized water. For coating the UCNP@RB-Pt/RNP NPs with cRGD-free liposome, the synthesis method was consistent with the UCNP@RB-Pt/RNP@liposome NPs with slight modification, and the liposome was replaced with cRGD-free liposome.

**ROS measurment *in vitro***

To measure the ROS level *in vitro*, the $H_2$DCFDA probe was added into 3 mL of PBS solution containing 600 μg URL to form a final concentration of 10 μM. After irradiated with 808 nm or 980 nm laser (0.5 W/cm$^2$, 5 min), the ROS levels of solution was monitored by the fluorescence of DCF (excitation at 488 nm).

**Cell culture**

HCT-116 cells (a human colorectal carcinoma cell line) and HCT116/L-OHP cells (an oxaliplatin-resistant colon cancer cell line) were cultured in RPMI 1640 supplied with 10% fetal bovine serum (FBS) and penicillin-streptomycin solution at 37 °C under an atmosphere containing 5% $CO_2$. HCT116 cells line was obtained from Shanghai Cell Bank. HCT116/L-OHP cells line was purchased from BeNa Culture Collection (BNCC) (catalog: BNCC353646).

**Detection of intracellular GSH**

After HCT116/L-OHP cells were seeded in a plate, URL NPs (100 μg/mL) were added into the 5 mL fresh medium and incubated for 4 h. Then, $10^7$ cells were collected and washed with PBS solution twice, followed by 808 nm/980 nm laser treatment (0.5 W/cm$^2$, 5 min). Finally, the Micro Reduced Glutathione (GSH) Assay Kit was used to detect the concentration of GSH according to the user's instructions and the maximum absorbance at 412 nm were recorded.

**Detection of intracellular ROS**

HCT116/L-OHP cells were seeded in glass-bottom dishes and then incubated with URL (200 μg/mL) for 4 h. After cells were washed with PBS solution twice, fresh medium containing 10 μM of Reactive Oxygen Species Assay Kit (Beyotime Biotechnology) was added. After incubation for 20 min at 37 °C, the dishes were washed with PBS solution twice and irradiated by an 808 nm laser (0.5 W/cm$^2$) or 980 nm laser (0.5 W/cm$^2$) for 5 min. Finally, confocal laser scanning microscope (CLSM) was utlized to observe the fluorescence of DCF (excitation at 488 nm).

**The tumor spheres model**

To construct 3D spheroid cell models, 3,000 cells were seeded a in 3D Corning™ ultra-low adhesion spheroid microplates (96-well) (CLS4520 Corning™, MA) per well. Then the cells were centrifuged at 1,000 rpm for 4 min and incubated for several days until 3D spheroid cell models were created.

**Cellular uptake of the UCNP@RB-Pt/RNP@liposome NPs**

Cellular uptake of URL was first examined using HCT116/L-OHP cells and tumor spheres. A total of $1.0 \times 10^5$ cells were cultured in confocal petri dishes for 12 h. Then, URL were added into this medium (100 μg/mL) and further incubated at 37 °C for 2 h, 4 h, and 8 h. After the cells were harvest and washed with PBS solution twice, the cells were resuspended in PBS and then subjected to flow cytometry. On the other hand, after being stained with Hoechst 33342 solution, the cells rinsed with phosphate buffered

saline (PBS) solution twice. Finally, before being imaged with a confocal scanning laser microscope (CLSM), the cells were fixed with 4% (wt/wt) paraformaldehyde for 15 min at RT.

To examine the targeting ability of the URL NPs, tumor spheres were picked into confocal petri dishes. After 1 mL of fresh medium containing URL (100 μg/mL) were added into those dishes and incubated for 4 h, the medium was replaced with PBS solution. Finally, after the tumor spheres were fixed with 4% (wt/wt) paraformaldehyde for 15 min at RT, the cellular uptake was imaged with a CLSM. (The emission was fixed at 570 nm).

### *In vitro* cell proliferation

To investigate the cytotoxicity of URL, oxaliplatin-resistant HCT116/L-OHP tumor cells were seeded in 96-well plates (2,000 cells per well) for 12 h. Then, 100 μL of medium containing different concentrations URL were added and incubated with 24 h. The MTT [3-(4,5)-dimethylthiahiazo (-z-y1)-3,5-di-phenytetrazoliumromide] assay (0.5 mg/mL) was utilized to evaluate the cytotoxicity of URL. Then, 200 μL of MTT assay was added to each well and incubated at 37 °C for 4 h. At the end, MTT solution was removed, and 200 μL dimethyl sulfoxide (DMSO) was added to dissolve the crystals. The absorbance of each well at 490 nm was measured to determine the cell viability.

### Western blotting

The protein of cells with different treatments was extracted with RIPA Lysis Buffer (Nanjing Vazyme Biotech Co., Ltd.) and quantified with BCA Protein Assay Kit (Sangon Biotech Co., Ltd.). A total of 20 μg protein was separated by SDS-PAGE on 10% polyacrylamide gel and then transferred to polyvinylidene fluoride membranes. Then, the membrane was blocked with 5% nonfat dry milk in 1 × Tris Buffered Saline with Tween 20 (TBST) buffer for 1 h at 37 °C. After the blots were incubated with the primary antibody at 4 °C overnight and incubated with secondary antibody at RT for 1.5 h, the membranes were washed with TBST solution for five times. Finally, protein bands were visualized by using ECL detection kit (Nanjing Vazyme Biotech Co., Ltd.) and imaged by using Chemi-luminescent Imaging System. The primary antibodies were: Anti-Bcl-2 Rabbit pAb (1:1,000; #GB113375, G SERVICEBIO), Anti-human β-Actin antibody (1:1,000; #8457T, Cell Signaling Technology), Anti-E-Cadherin Rabbit pAb (1:1,000; #GB11082, G SERVICEBIO), Anti-N-Cadherin Mouse mAb (1:1,000; #GB12135, G SERVICEBIO), MRP1 Mouse Monoclonal Antibody (1:5,000; #67228-1-Ig, Proteintech Group, Inc.), Anti-human P53 antibody (1:1,000; #2527T, Cell Signaling Technology), AKT (phosphor-S473) polyclonal antibody (1:500; #BS4007, Bioworld Technology, Inc), AKT1 pAb Rabbit antibody (1:1,000; #AP0059, Bioworld Technology, Inc), and Anti-Bax Rabbit pAb (1:500; #GB11690, G SERVICEBIO). The secondary antibodies were horseradish peroxidase (HRP)–conjugated anti-rabbit antibodies (1:1,000; #7074P2, Cell Signaling Technology), and horseradish peroxidase (HRP)–conjugated anti-mouse antibodies (1:5,000; Santa Cruz Biotechnology).

### Immunofluorescence analysis

HCT116/L-OHP cells were seeded on cell climbing films for 12 h. After the URL (100 μg/mL) were added in the 1 mL of medium and incubated for 4 h, the cells were irradiated with 808 nm laser or 980

nm laser (0.5 W/cm$^2$) for 5 min. After 12 h of incubation, the cells were fixed with 4% (wt/wt) paraformaldehyde for 15 min at RT. Before blocked with 10% bovine serum albumin (BSA) for 1 h at 37 °C, the cells were permeabilized with 0.2% Triton X-100 for 10 min. The cells were incubated with MRP1/ABCC1 Rabbit pAb (1:50; #A3027, ABclonal) overnight and then incubated with the IgG H&L (Alexa Fluor® 488) (1:200; #ab150077, Abcam) for 1 h. After the nucleus were stained with Hoechst 33342 (Invitrogen) for 10 min, the slides were visualized with a CLSM.

**Real-time PCR**

Total RNA was extracted from cultured cells undergoing different treatments using TRIZOL Reagent and UNIQ-10 Column Trizol Total RNA Isolation Kit (Sangon Biotech Co., Ltd.) according to the manufacturer's instructions. Then, RNA was quantified spectrophotometrically using a NanoDrop 2000 spectrophotometer (Thermo Scientific, USA). cDNA was generated from 1 μg of total RNA using HiScript III RT SuperMix for qPCR (+ gDNA wiper) (Nanjing Vazyme Biotech Co., Ltd.), and mRNA level was determined using AceQ qPCR SYBR® Green Master Mix (Without ROX) (Nanjing Vazyme Biotech Co., Ltd.) according to the manufacturer's instructions. The 2^ΔΔCT method was used to determine the relative expression levels and we quantified β-Actin levels as an endogenous control. All assays were performed in triplicate, and the sequence of primers were listed in **Table S1**.

**Confocal imaging of TUNEL staining**

HCT116/L-OHP cells were seeded on confocal petri dishes and incubated for 12 h. The medium was replaced by 500 μL of fresh medium containing URL (100 μg/mL) and incubated for 4 h. Then the cells were treated with different treatments and washed with PBS solution twice, and fixed with 4% paraformaldehyde for 15 min at RT. After the cells were stained with YF®488 TUNEL Apoptosis Kit (Green Fluorescence) (US EVERBRIGHT, Suzhou, China) according to the manufacturer's protocols for CLSM detection, nuclei were stained with Hoechst 33342 solution.

**Apoptosis analysis by flow cytometry**

HCT116/L-OHP cells were seeded in six-well plates (5 × 10$^5$ cells per well) and incubated for 12 h. The medium was replaced by medium containing URL and incubated for 4 h. Then cells were irradiated with 980 nm laser or 808 nm laser for 5 min (0.5 W/cm$^2$). After incubating for another 12 h, the cells in the URL + 980 + 808 nm group and URL + 808 + 980 nm group were irradiated with 808 nm or 980 nm separately. After incubating for 12 h, the cells were harvest and washed with PBS solution twice and stained by YF®488-Annexin V/RedNucleus II Apoptosis Kit (US EVERBRIGHT, Suzhou, China) according to the manufacturer's instructions.

**Cell migration and invasion assays**

HCT116/L-OHP cells were cultured in 6-well microplates for 24 h. After 1 mL of URL (100 μg/mL) were added into 6-well microplates and incubated for 4 h, the cells were treated with irradiation. Then a wound was scratched on the confluent cell monolayers with a 200 μL pipette tip. The cells were washed with PBS solution for twice and cultured in fresh medium for 48 h. The wound healing was photographed by

microscope.

Transwell assays were used to evaluate *in vitro* cell migration. Firstly, matrigel coated trans-well polycarbonate filters (pore size: 8.0 μm) (CORNING Biosciences) were prepared. Then the cells were incubated with URL and were treated with irradiation. Then 200 μL of serum-free RPMI 1640 medium containing $5 \times 10^4$ cells from different groups were added into the upper chambers, and 700 μL of fresh RPMI 1640 medium containing 20% FBS was placed in the lower chambers. After incubation at 37 °C for another 48 h, the cells were fixed with 4% (wt/wt) formaldehyde for 10 min at RT, then the inserts were fixed and stained with crystal violet. The non-invasive cells in the upper chambers were removed by using cotton swabs and cells on the lower surface were photographed with a microscope.

**Animal model**

Nude mice (18 ± 2 g, 6-8 weeks old) were purchased from the Changzhou Cavens Laboratory Animal Ltd,. All animal experiments were approved by the Animal Care and Use Committee of Nanjing University (IACUC-2204011). When the tumors reached ~100 $mm^3$, mice bearing tumors were used for imaging as well as treatment.

***In vivo* and *ex vivo* fluorescence imaging**

*In vivo* fluorescence images were acquired at different time points after a tail vein injection of the 100 μL of PBS containing URL (200 μL/mL) with or without cRGD by using a *In Vivo* Imaging Systems (IVIS). Finally, main organs were isolated and imaged (excited at 570 nm).

***In vivo* anti-tumor experiment**

When tumors reached a mean volume of about 100 $mm^3$, the nude mice were divided into six groups (three mice per group) randomly (i.e., PBS group, URL group, URL + 980 nm group, URL + 808 nm group, URL + 980 + 808 nm group, and URL + 808 + 980 nm group). After intravenously administered 100 μL of PBS containing URL (200 μg/mL) for 4 h, the mice were exposed to 808/980 nm laser (0.5 $W/cm^2$) for 5 min. After 12 h, the tumor was irradiated with 808 nm or 980 nm laser again (0.5 $W/cm^2$, 5 min). 24 hour later, the tumors were evaluated by ROS staining and MRP1 immunofluorescence staining. The tumor volume was recorded every 2 days. Finally, at the time of sacrifice, the mice were dissected to excise organs and tumors to evaluate the therapeutic efficacy by cell proliferation and apoptosis, E-cadherin, and N-cadherin immunofluorescence staining. The volume calculations were obtained using the formula $V = (\text{length} \times \text{width}^2)/2$. The growth inhibition rate of tumors was calculated according to the following formula: the tumor growth inhibition (TGI) = [1-RTV (treatment group)/ RTV (control group) × 100%], $RTV=V_t/V_0$ [$V_t$: The volume of the (treatment group) tumor at the end of an experimental cycle; $V_0$: The volume of the tumor at the beginning of the experiment].

**Statistical analysis**

All data were analyzed using GraphPad Prism 8.4. Statistical analysis was carried out by student's test and one-way ANOVA for comparison of two groups. Data were presented as mean ± SE. *$p < 0.05$, **$p < 0.01$, ***$p < 0.001$, ****$p < 0.0001$, ns: not significant.

## Supplemental Figures

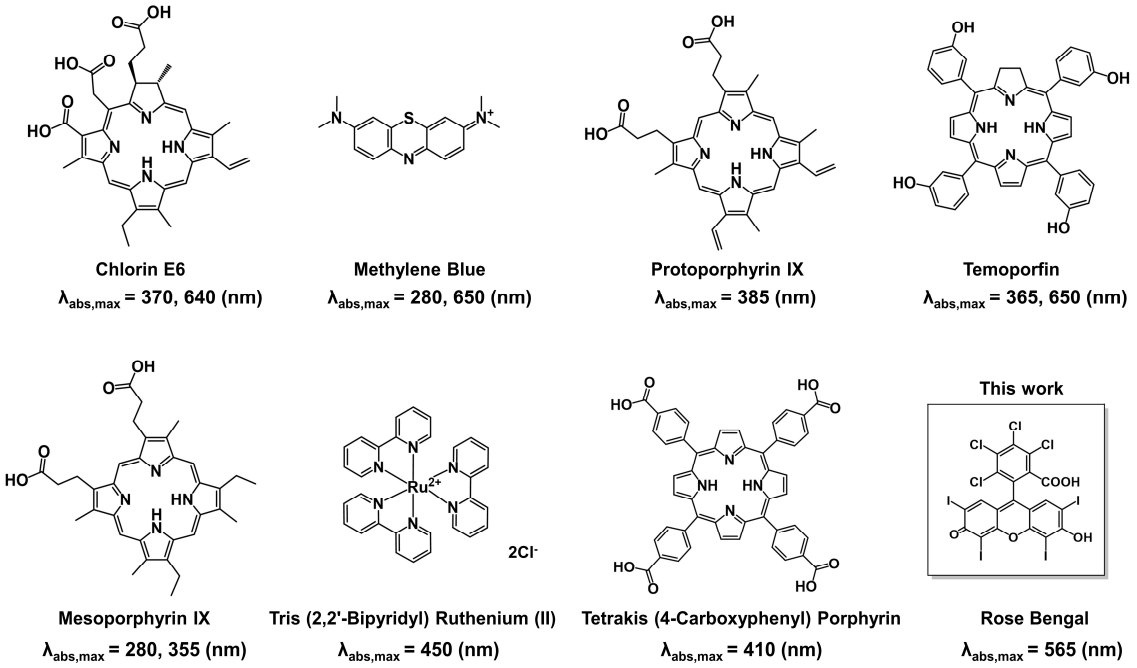


**Figure S1**. Chemical structure and maximum absorption wavelength of the photosensitizers.

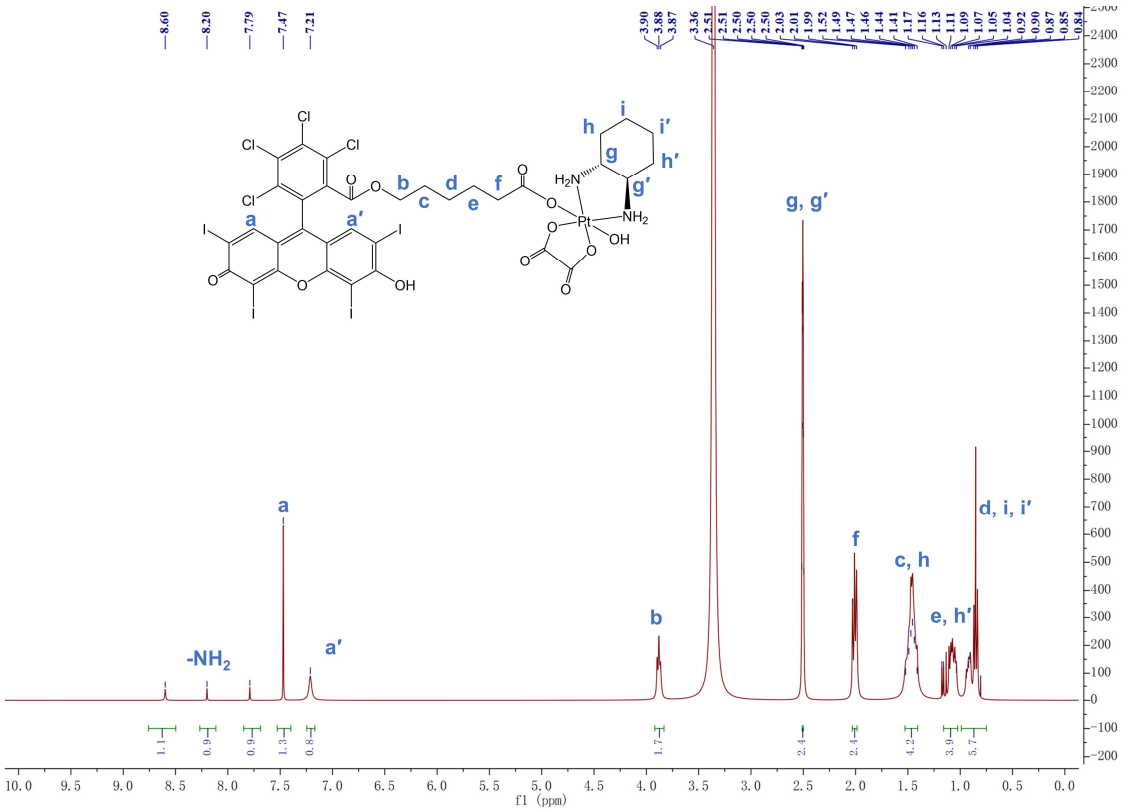


**Figure S2**. $^{1}$H-NMR spectrum of RB-Pt in $(CD_3)_2SO$.

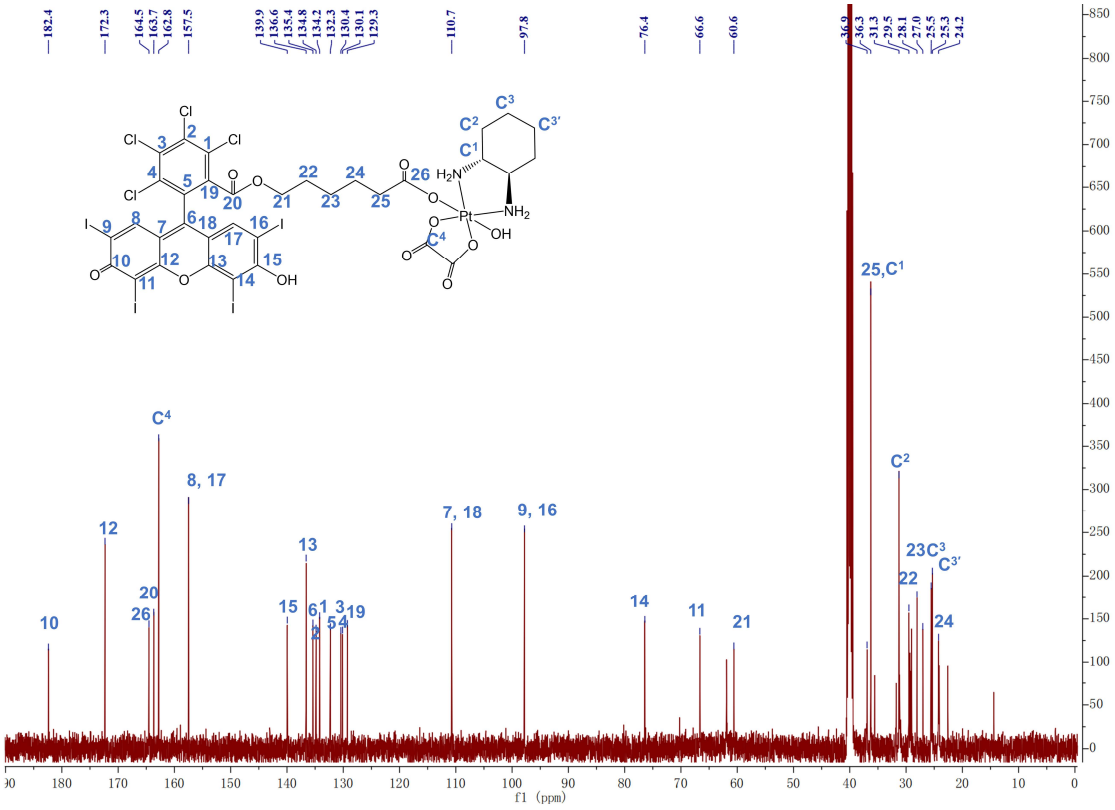


**Figure S3**. $^{13}$C-NMR spectrum of RB-Pt in $(CD_3)_2SO$.

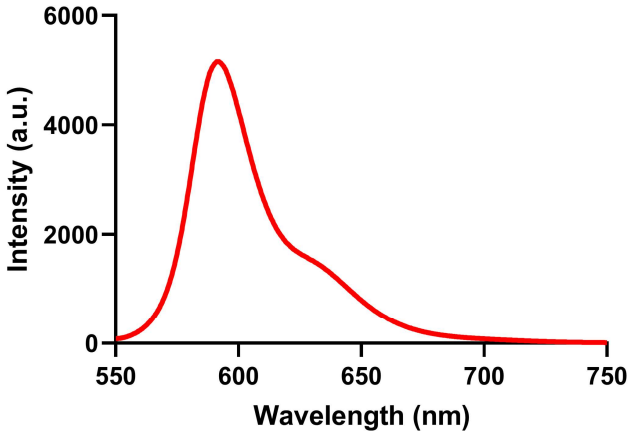


**Figure S4**. Fluorescence spectra of RB-Pt with excitation wavelengths of 540 nm.

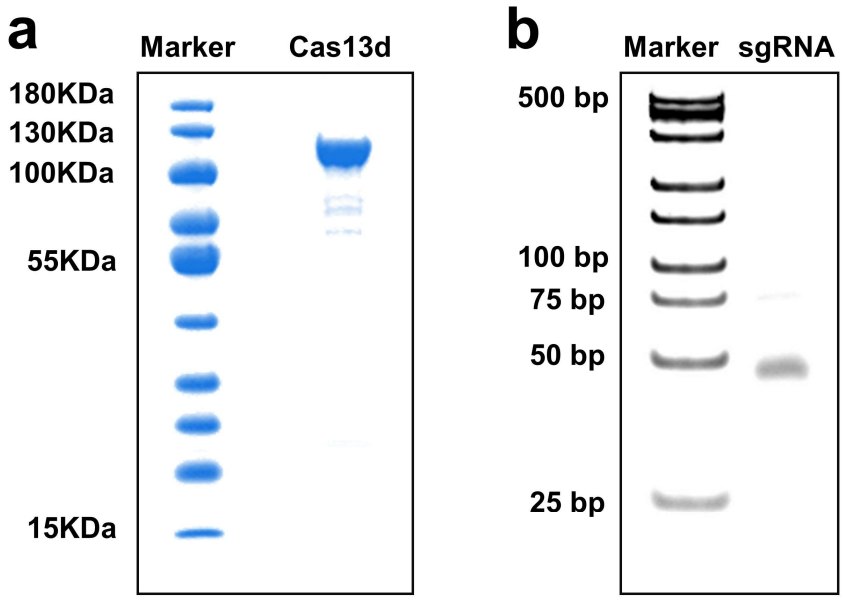


**Figure S5**. (a) SDS-polyacrylamide gel electrophoresis (SDS-PAGE, 10%) analysis of the purified RspCas13d. (b) Gel Red stain of an 8 M urea 10% polyacrylamide gel with purified sgRNA.

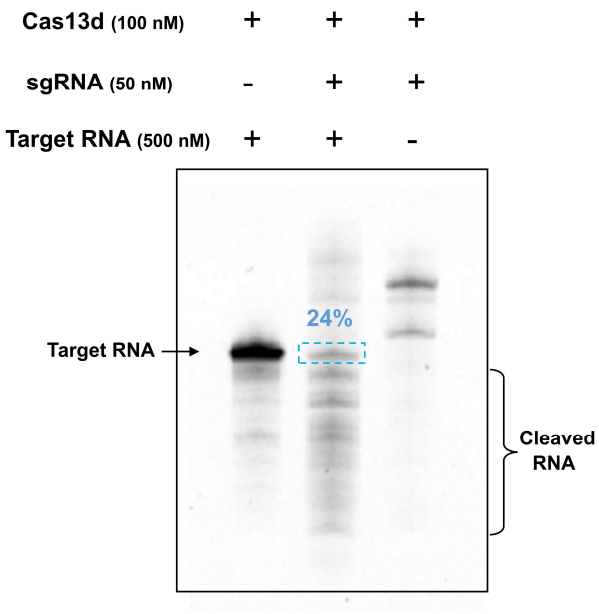


**Figure S6.** Gel Red stain of an 8 M urea 10% polyacrylamide gel with target RNA to test the cleavage efficiency of Cas13d/sgRNA.

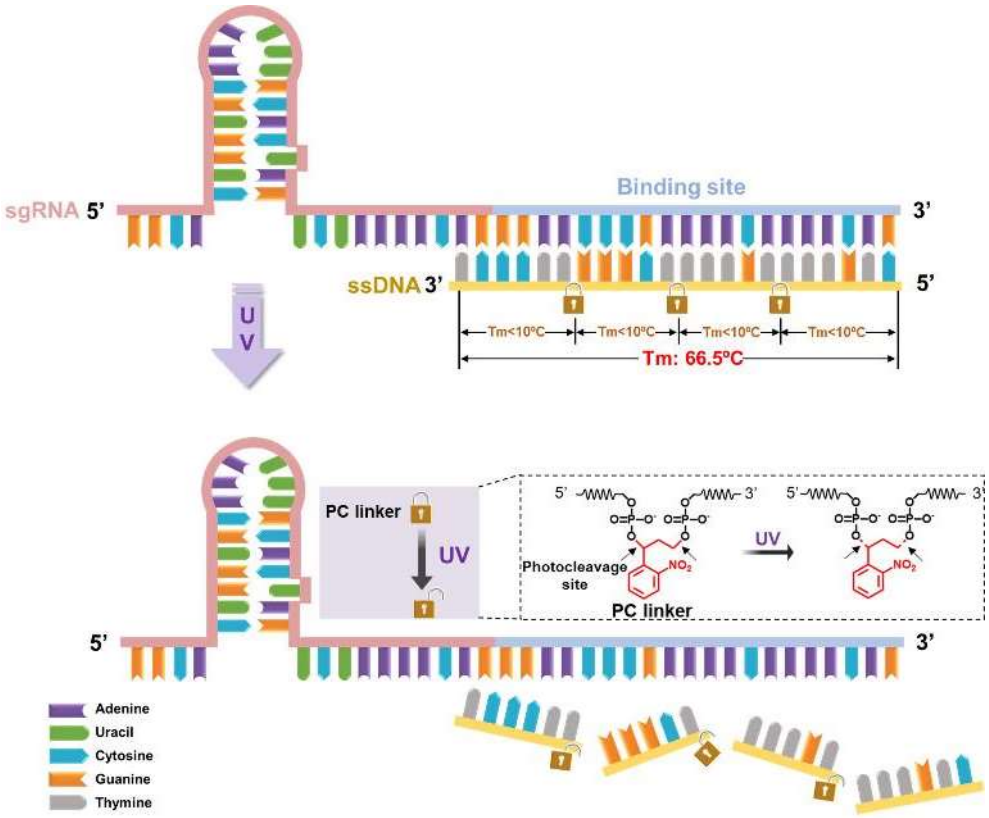


**Figure S7**. Schematic diagram of Cas13d-based sgRNA blocked by single strand DNA (ssDNA) and activated by ultraviolet light to knockdown MRP1 mRNA.

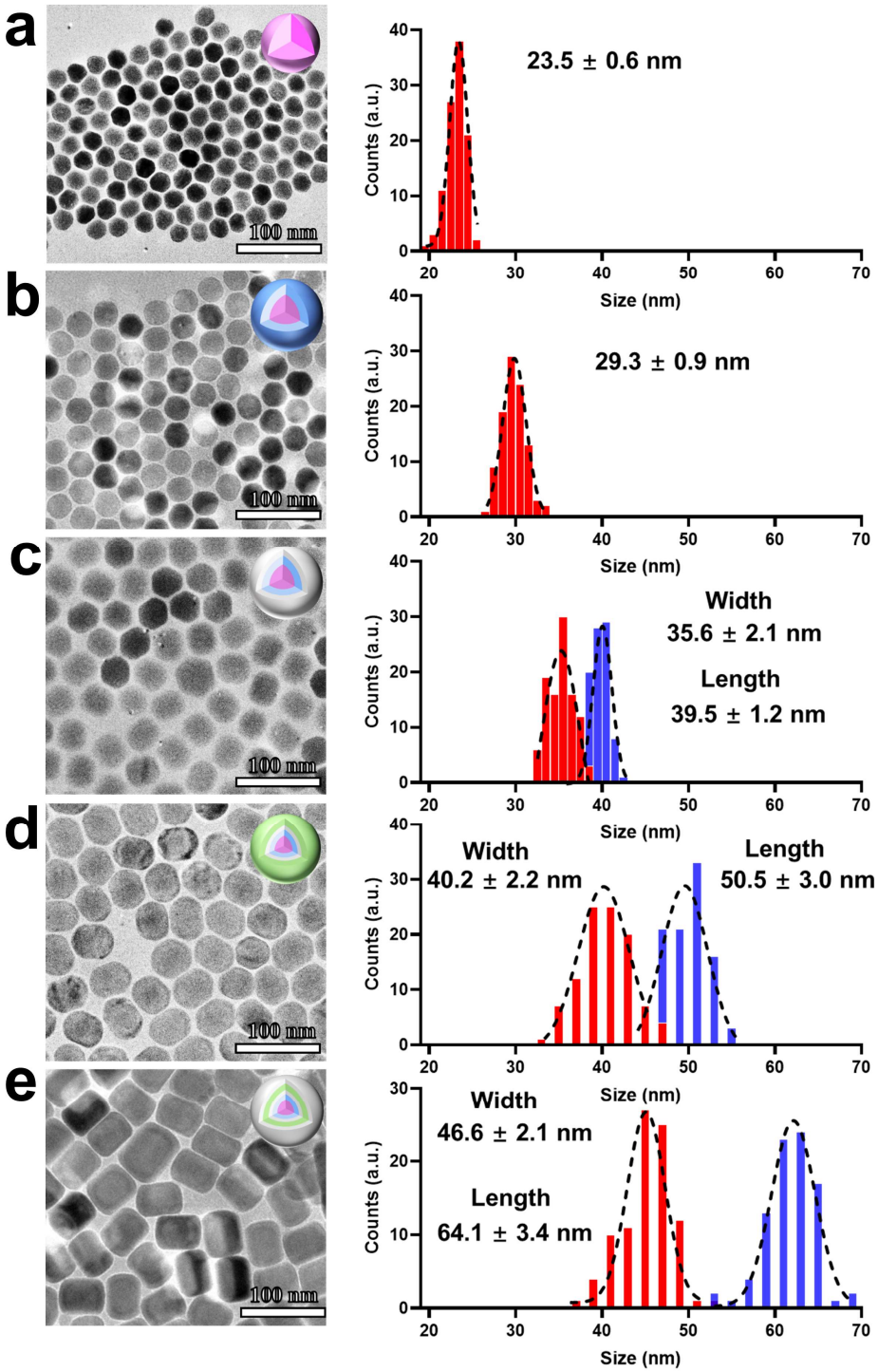


**Figure S8.** TEM and corresponding size distribution of the starting core and core/multi-shell UCNPs. (a) the starting core (NPs, $NaYF_4$:20%Nd/20%Yb), (b) core@shell NPs (CS-NPs, $NaYF_4$:20%Nd/20%Yb@$NaYF_4$: 30%Yb/0.5%Tm), (c) core@shell@shell NPs (CSS-NPs, $NaYF_4$:20%Nd/20%Yb@$NaYF_4$:30%Yb/0.5%Tm@ $NaYF_4$), (d) core@shell@shell@shell NPs (CSSS-NPs, $NaYF_4$:20%Nd/20%Yb@$NaYF_4$:30%Yb/0.5%Tm@ $NaYF_4$@$NaYbF_4$:1%Ho), and (e) the final core@shell@shell@shell@shell NPs (UCNPs, $NaYF_4$:20%Nd/20%Yb @$NaYF_4$:30%Yb/0.5%Tm@$NaYF_4$@$NaYbF_4$:1%Ho@$NaYF_4$).

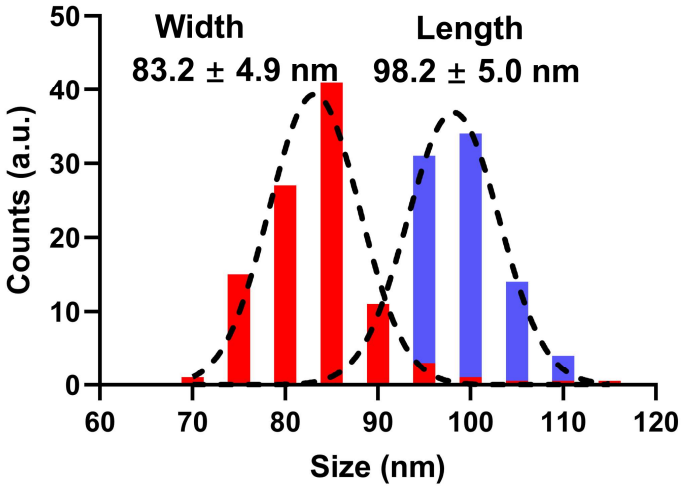


**Figure S9.** Size distribution of the UCNP@mSiO$_2$.

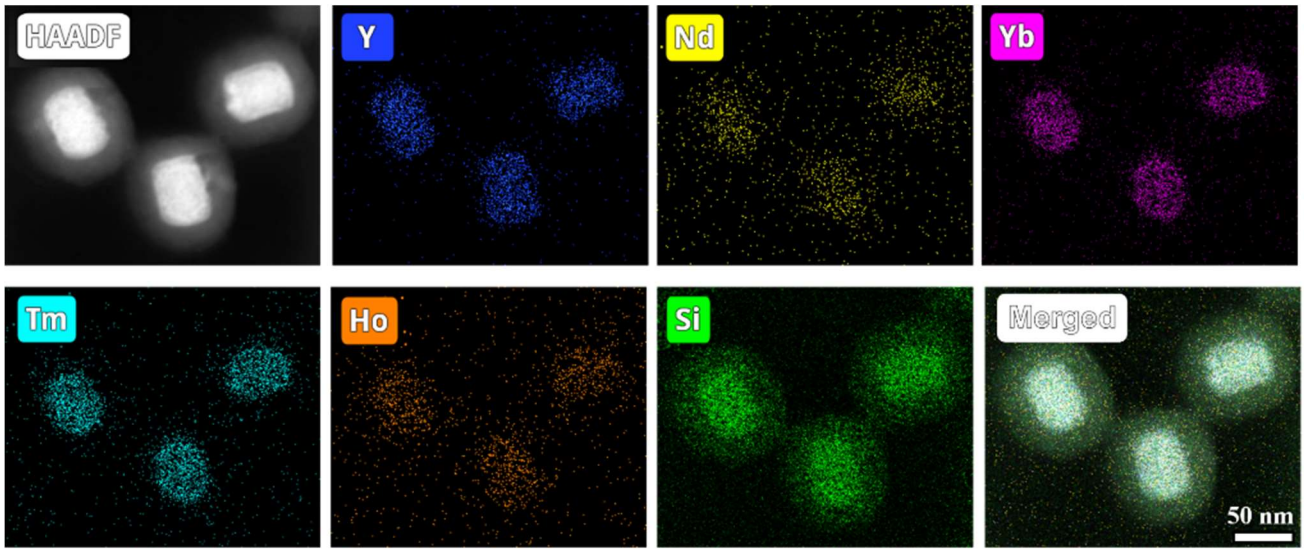


**Figure S10.** Structural and compositional characterization of the UCNP@mSiO$_2$. High-angle annular dark-field (HAADF) image and corresponding elemental mapping results displayed a clear core-shell geometry and homogeneous distribution of Y, Nd, Yb, Tm, Ho, and Si within the UCNP@mSiO$_2$, confirming the successful core/multi-shell construction.

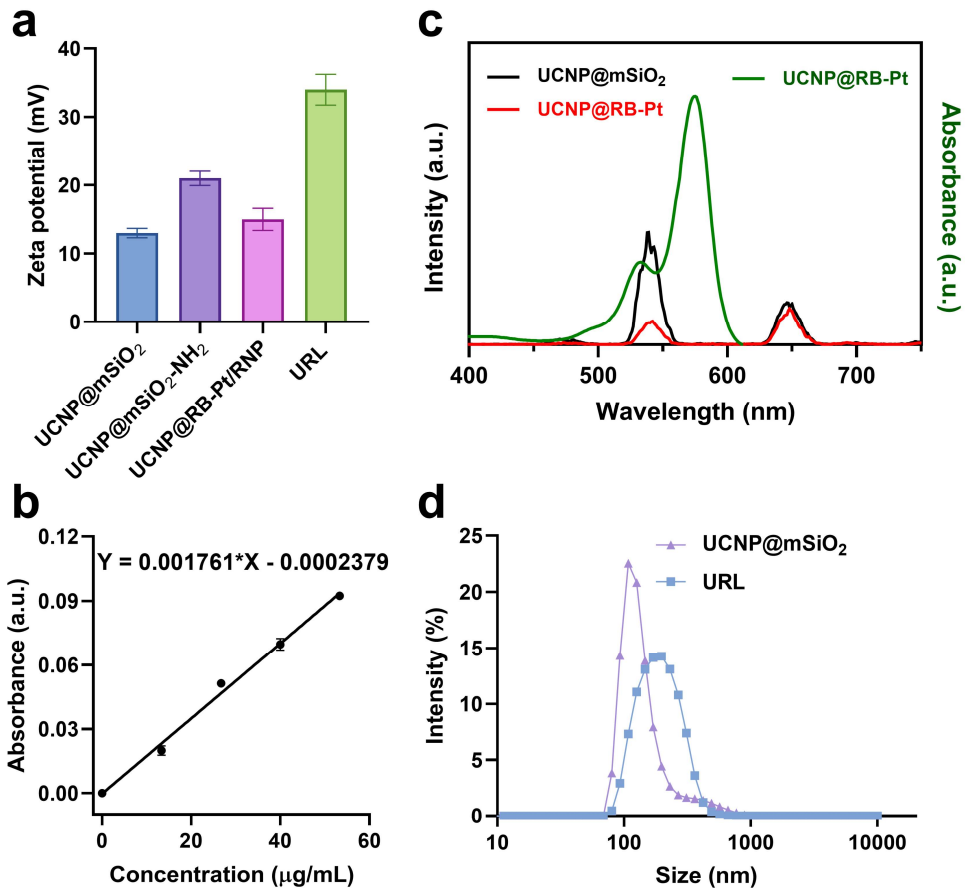


**Figure S11.** Characterization of the URL nanoprodrug. (a) Zeta potential analysis of UCNP@$mSiO_2$, UCNP@$mSiO_2$-$NH_2$, UCNP@RB-Pt/RNP and UCNP@RB-Pt/RNP@liposome-cRGD NPs (URL). (b) Linear regression curve of the RB-Pt concentration vs UV-vis absorbance peak at 575 nm. The characteristic peaks of benzene rings and rigid coplanar π-Conjugated skeleton for RB-Pt were detected, and the prodrug loading capacity of UCNP@$mSiO_2$@RB-Pt was calculated to be 67 mg/g. (c) Both UCNP@$mSiO_2$ and UCNP@$mSiO_2$@RB-Pt maintained the unique UCL properties from the UCNPs, whereas the visible green UCL band of the latter under 980-nm irradiation overlaped well with the absorbance spectra of RB-Pt prodrug. Such a feature meets our expectation of reaching a wavelength-selective prodrug activation through NIR UCL emission. UV–vis absorption spectra of RB-Pt (green line), up-conversion emission spectra of UCNPs (black line) and UCNP@$mSiO_2$@RB-Pt NPs (red line) exposed to a 980-nm laser. (d) Hydrodynamic diameters of UCNP@$mSiO_2$, and URL measured by dynamic light scattering method.

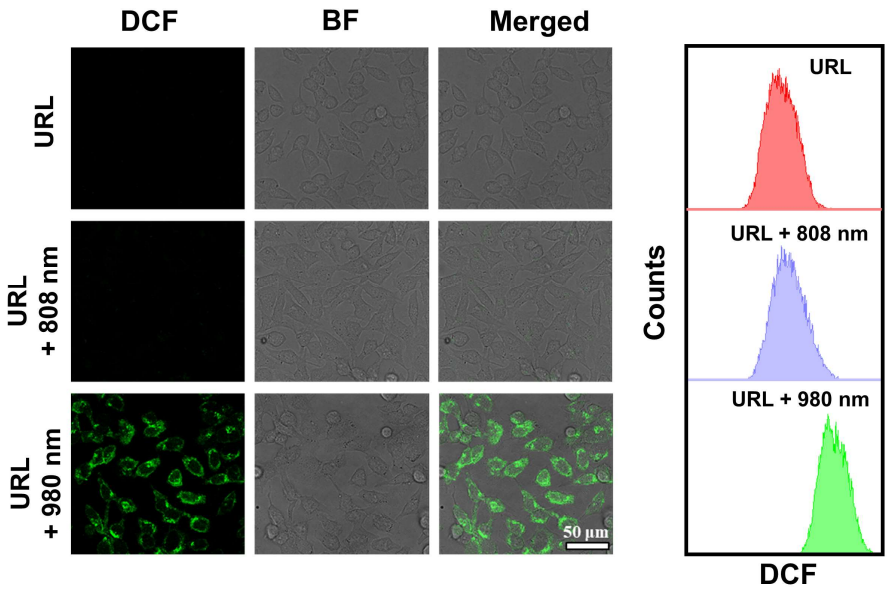


**Figure S12.** CLSM images and flow cytometry assay of $H_2$DCFDA-stained HCT116/L-OHP cells post-incubation with URL for 4 h followed by irradiation at 808 nm or 980 nm (0.5 W/cm$^2$) for 5 min ($E_x$ = 488 nm, $E_m$ = 500-550 nm).

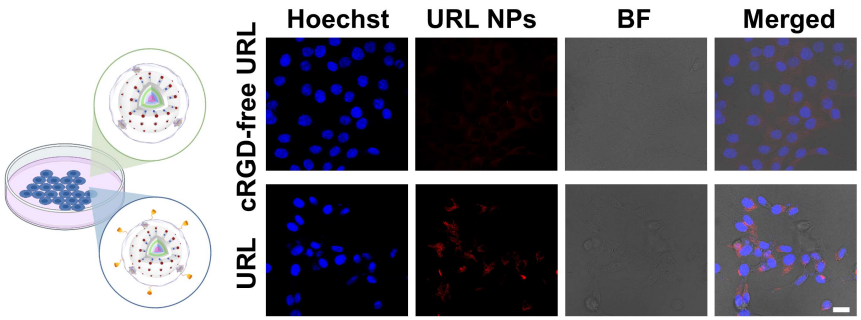


**Figure S13.**. Representative CLSM images of HCT116/L-OHP cells post-incubation with cRGD-free URL or URL for 4 h. Scar bar: 20 μm. To demonstrate the role of the cRGD moiety in guiding URL to αvβ3 integrin-rich tumor cells, αvβ3-positive colorectal cells were incubated with URL bearing cRGD and cRGD-free URL at 37 °C for 4 h. Confocal fluorescence microscopy images demonstrated that bright red fluorescence was distributed evenly in the cytoplasm of cell treated with cRGD-modified URL, while negligible red fluorescence was observed in cRGD-free URL group following an identical protocol. These observations confirmed the specific interaction between cRGD-modified URL and αVβ3 integrin overexpressed on tumor cells

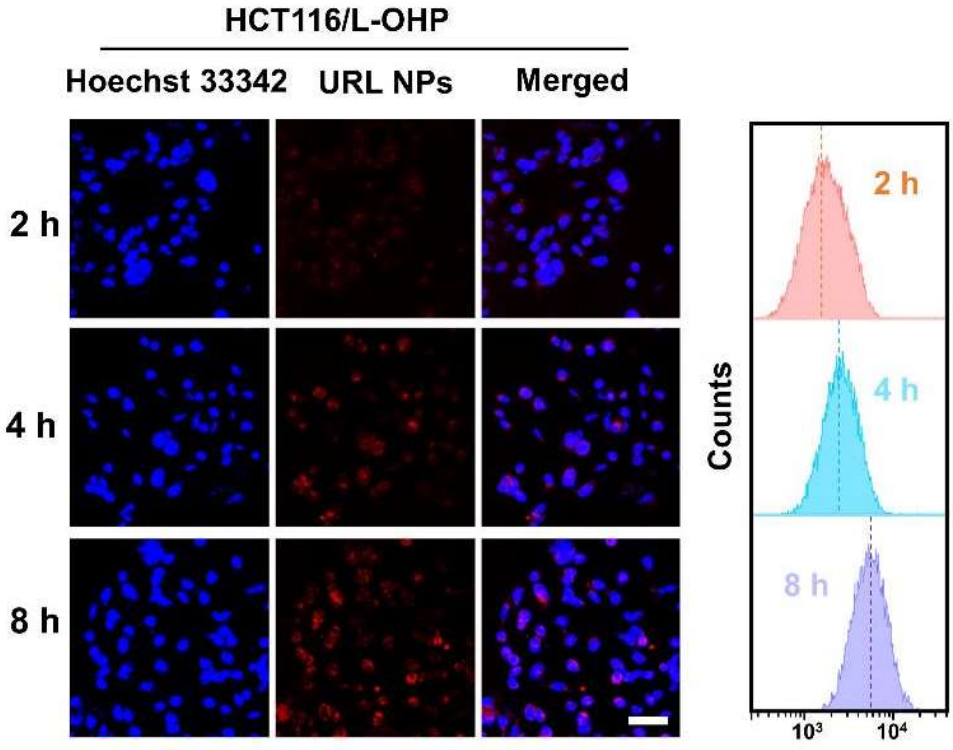


**Figure S14.** CLSM images and flow cytometry assay of HCT116/L-OHP cells post-incubation with URL for 2, 4, and 8 h. The blue fluorescence is from Hoechst 33342, and the red fluorescence is from RB-Pt. Scar bar: 50 μm. The time-dependent internalization of URL was evaluated by confocal fluorescence microscopy. An obvious cytoplasmic accumulation of URL could be observed as early as 2 h and remained increased thereafter, which were further confirmed by flow cytometric analysis.These findings indicated that the introduction of cRGD improved the cellular uptake efficiency of URL.

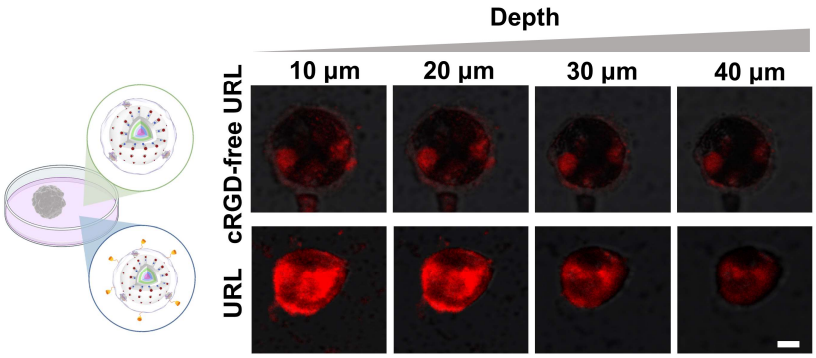


**Figure S15.** Tumor targeting and penetration behavior of URL. Representative CLSM images of tumor cell spheres post-incubation with cRGD-free URL or URL for 4 h. Scar bar: 50 μm.The penetration was monitored by measuring the fluorescence of the RB-Pt using CLSM. Compared with cRGD-free URL group, cRGD-modified URL consistently displayed bright and higher fluorescence signal throughout the tumor sphere section at different depth levels, suggesting enhanced penetration.

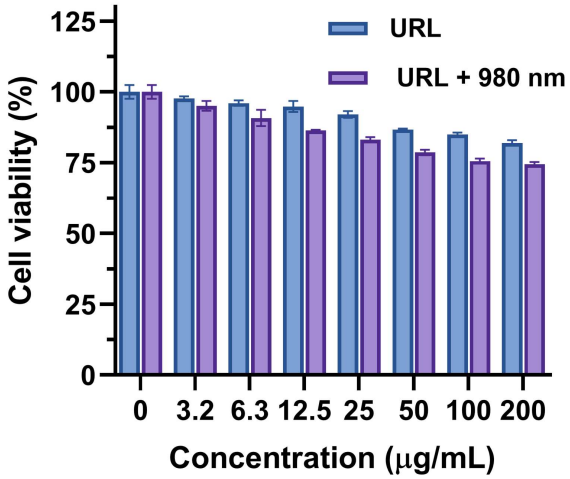


**Figure S16.** Cell viability of HCT116/L-OHP cells post-incubation with different concentrations of URL followed by 980-nm light irradiation for 5 min.

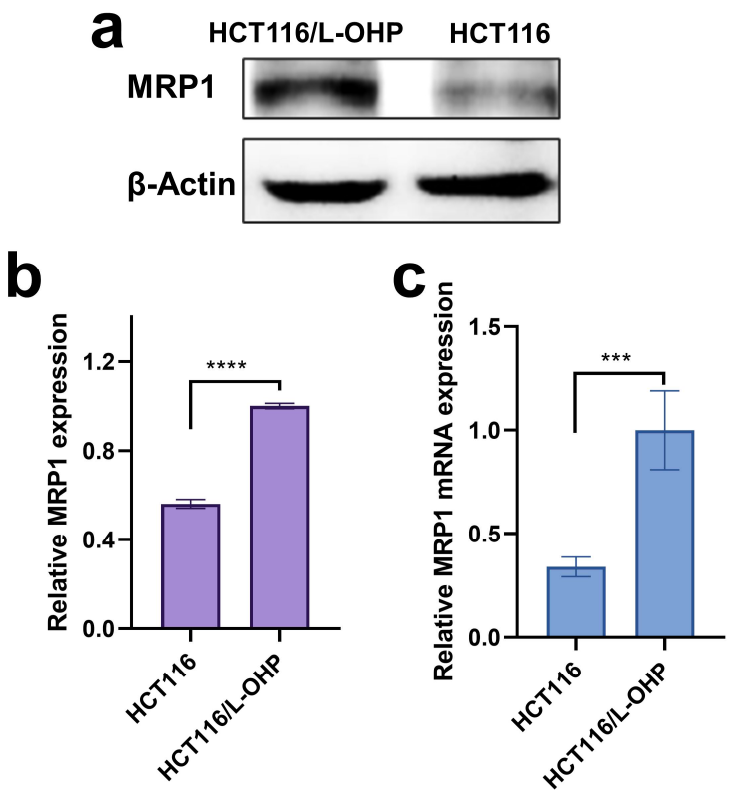


**Figure S17.** Comparison of MRP1 expression in HCT116 and HCT116/L-OHP cells. (a) Western blot analysis of MRP1 expression in oxaliplatin-resistant HCT116/L-OHP cells and normal HCT116 cells. (b) Quantitative densitometric analysis of MRP1 levels shown in (a). Data are means ± SE (n = 3). (c) Comparision of relative MRP1 mRNA expression in HCT116/L-OHP and HCT116 cells. ***$p < 0.001$, ****$p < 0.0001$.

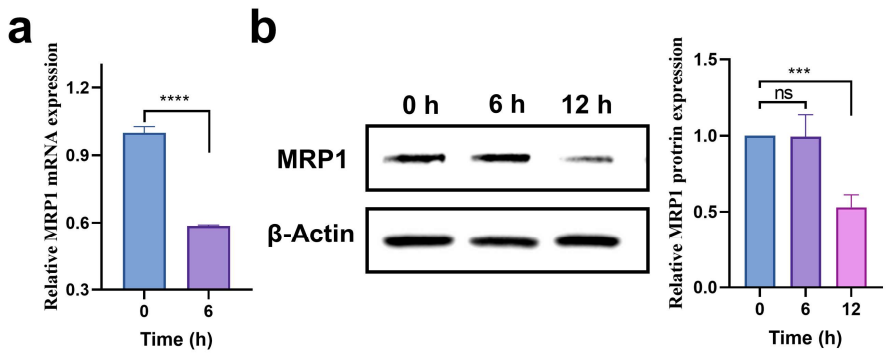


**Figure S18.** (a) Relative MRP1 mRNA expression in HCT116/L-OHP cells post-incubation with URL assembled using uncaged RNPs for the indicated time points. (b) Western blot analysis of MRP1 expression in HCT116/L-OHP cells post-incubation with URL assembled using uncaged RNPs for the indicated time points. And quantitative densitometric analysis of MRP1 levels. Data are means ± SE (n = 3). ***$p < 0.001$, ****$p < 0.0001$, ns: not significant.

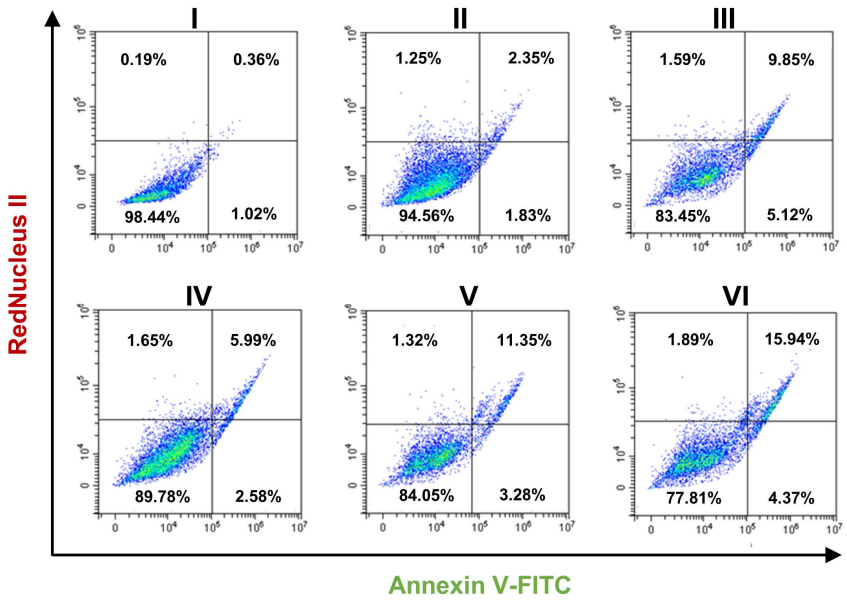


**Figure S19.** Flow cytometry analysis of apoptosis in HCT116/L-OHP cells after the indicated treatments, as determined by Annexin V–FITC/RedNucleus II double staining.

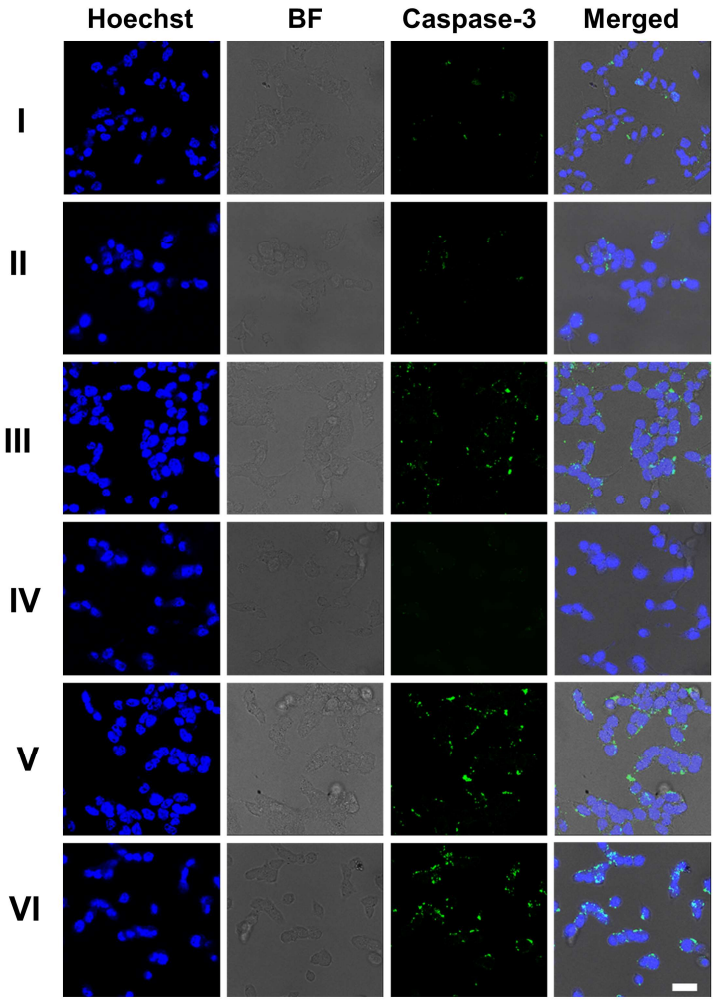


**Figure S20.** CLSM images of active caspase-3 staining of HCT116/L-OHP cells treated with indicated treatments. Active caspase-3 was detected by using GreenNuc™ Caspase-3 Assay Kit (green), while cell nuclei were stained with Hoechst 33342 (blue). Scale bar: 20 μm.

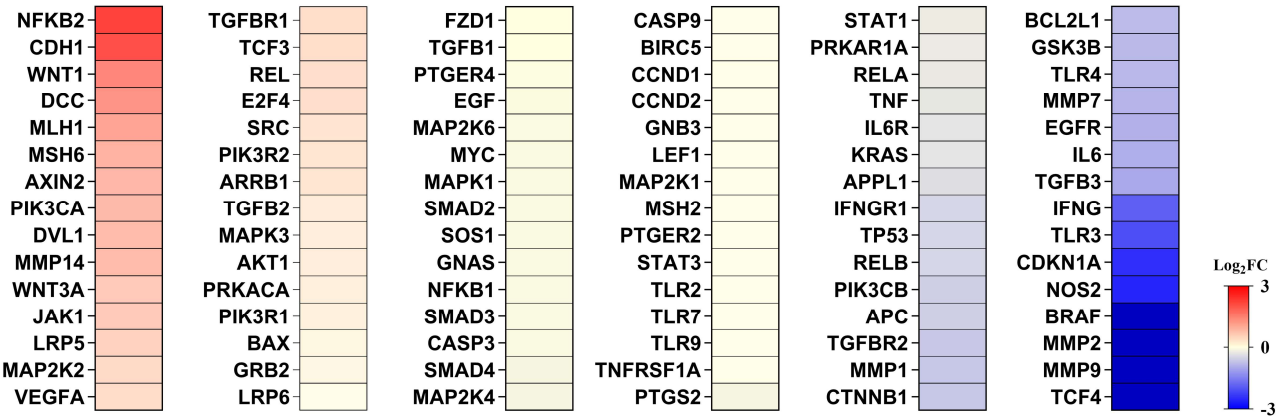


**Figure S21.** Effects of synergistic therapy on migration-related genes in HCT116/L-OHP cells. (a) PCR array heatmap of the EMT related genes expressed in HTC116/L-OHP cells post-incubation with URL for 4 h followed by sequential 808- and 980-nm irradiation (0.5 W/cm$^2$) for 5 min. PBS-treated HTC116/L-OHP cells were used as the negative control.

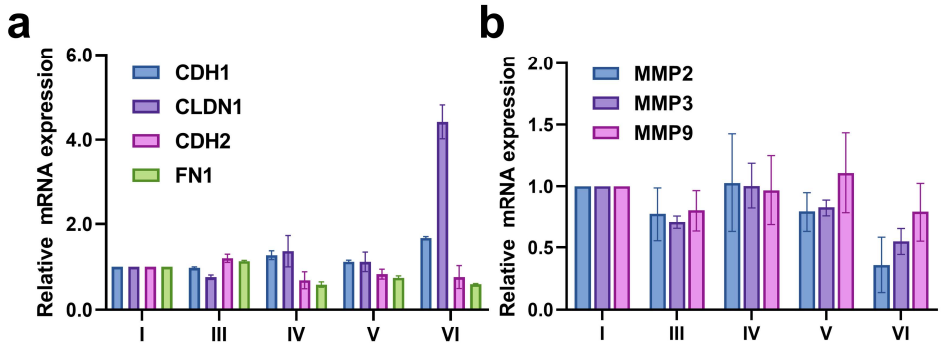


**Figure S22.** Relative expression of metastasis (a) and invasion (b) related mRNA in HCT116/L-OHP cells with the indicated treatments. Upregulation of the CDH1 (E-cadherin) and CLDN1 (epithelial markers claudin 1) but downregulation of CDH2 (N-cadherin) and FN1 (Fibronectin 1) indicates the inhibition of tumor metastasis. Downregulation of matrix metalloproteinase (MMP)-related mRNA, including MMP2, MMP3, and MMP9, indicates the inhibition of tumor cell invasion.

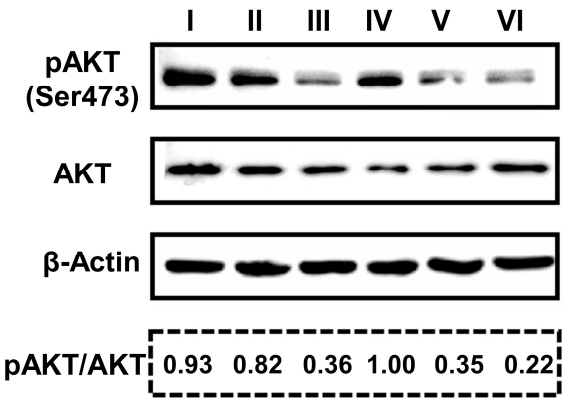


**Figure S23.** Western blot analysis of p-AKT(Ser473) and AKT expression in HCT116/L-OHP cells after the indicated treatments.

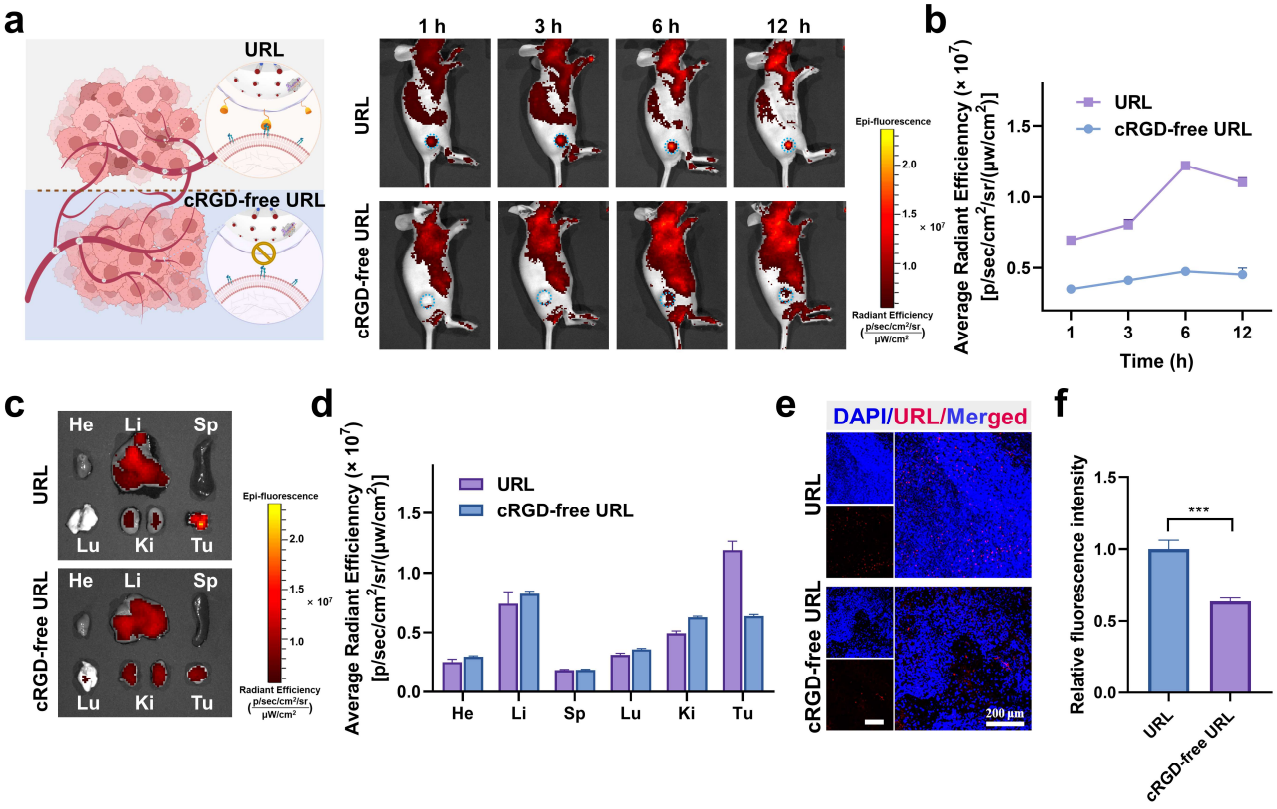


**Figure S24.** *In vivo* behavior of URL with or without cRGD modification. (a) *In vivo* fluorescence imaging of mice at different time points after intravenous injection of URL with or without cRGD modification. Blue circles indicate the locations of tumors. (b) The quantitative results of URL accumulated in tumors at different time point. (c) *Ex vivo* fluorescence images of major organs and tumors striped from those mice at 12 h after intravenous injection. He, Li, Sp, Lu, Ki, and Tu, stand for heart, liver, spleen, lung, kidney, and tumor, respectively. (d) Quantification of fluorescence signal at main organs in different mouse at 12 h after NPs injection. (e, f) Confocal images (e) and quantitative fluorescence analysis (f) showing the significant enrichment of cRGD-modified URL in tumor tissues. ***P < 0.001.

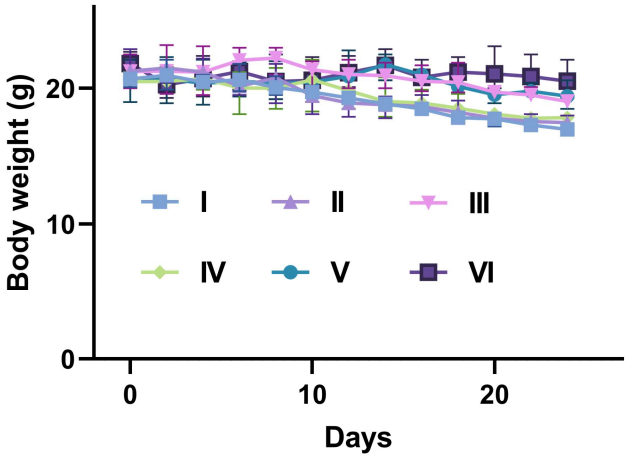


**Figure S25.** Body weight of each mice group. Each value is expressed as mean ± SE.

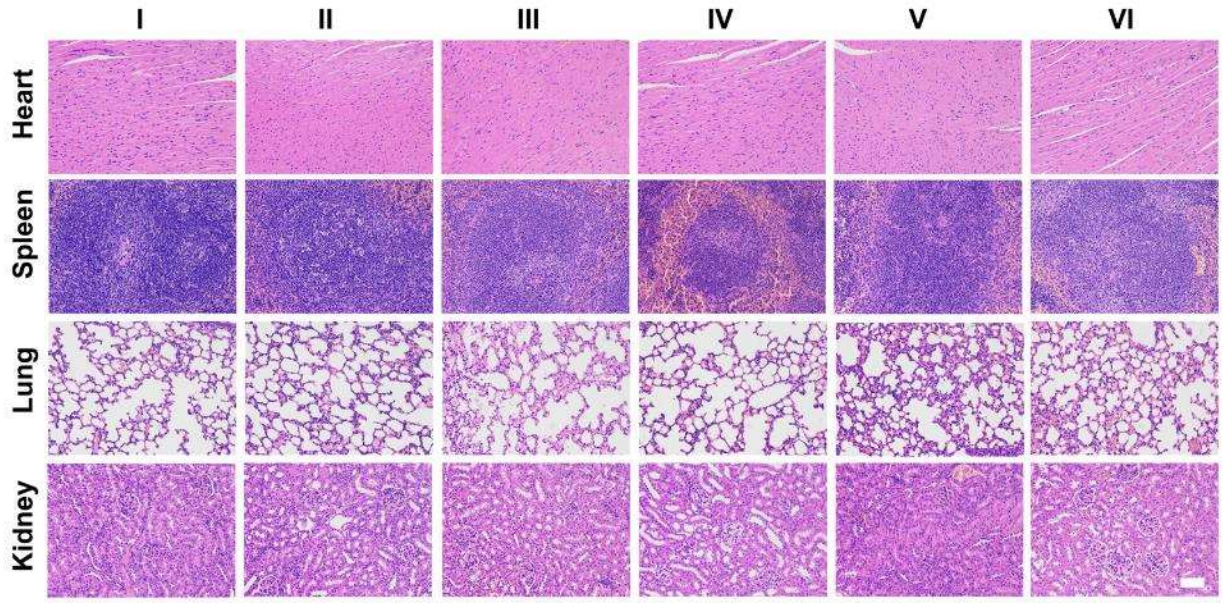


**Figure S26.** Microphotographs of H&E stained major organs at the end of different treatments. Scale bars: 100 μm.

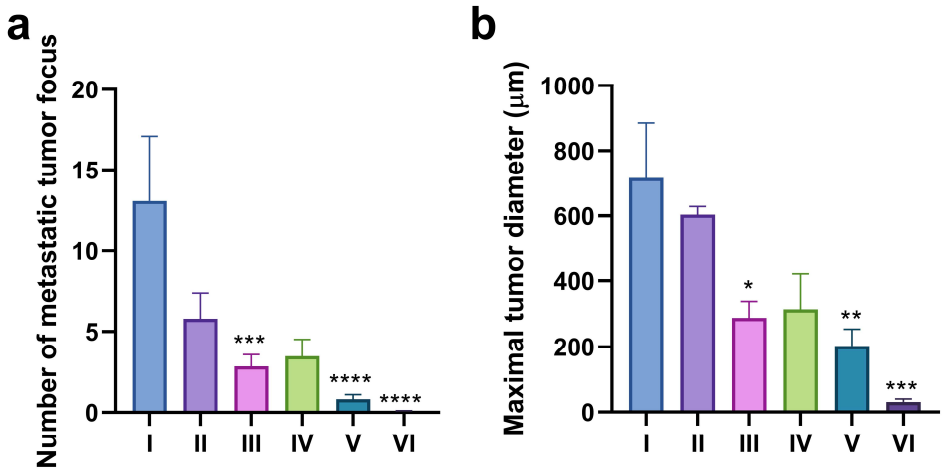


**Figure S27.** Orthogonally reversing chemoresistance for enhanced chemo-photodynamic therapy to inhibit liver metastases from colon cancer. Statistical analysis of the number of liver metastases (a) and the diameter of the largest liver metastases (b) at the end of treatment. *P < 0.05, **P < 0.01, ***P < 0.001 and ****P < 0.0001.

**Table S1. Sequences of the oligonucleotides used in our work**

| Note | Sequence (5'–3') |
|---|---|
| sgRNA-F | CTGTTTTGTTTTCGGGTTCCCTGTTTTAGACTAGTGCAAATTT GCACCAGTGCCTATAGTGAGTCGTATTA |
| sgRNA-R | CTGTTTTGTTTTCGGGTTCCCTGTTTTAGACTAGTGCAAATTT GCACCAGTGCCTATAGTGAGTCGTATTA |
| MRP1 sgRNA | GGCACUGGUGCAAAUUUGCACUAGUCUAAAACAGGGAACC CGAAAACAAAACAG |
| ssDNA | CTGTTT/iPCLink/TGTTT/iPCLink/TCGGG/iPCLink/TTCCCT |
| CDH1-F | GCCTCCTGAAAAGAGAGTGGAAG |
| CDH1-R | TGGCAGTGTCTCTCCAAATCCG |
| CLDN1-F | GTCTTTGACTCCTTGCTGAATCTG |
| CLDN1-R | CACCTCATCGTCTTCCAAGCAC |
| CDH2-F | CCTCCAGAGTTTACTGCCATGAC |
| CDH2-R | GTAGGATCTCCGCCACTGATTC |
| FN1-F | ACAACACCGAGGTGACTGAGAC |
| FN1-R | GGACACAACGATGCTTCCTGAG |
| MMP2-F | AGCGAGTGGATGCCGCCTTTAA |
| MMP2-R | CATTCCAGGCATCTGCGATGAG |
| MMP3-F | CACTCACAGACCTGACTCGGTT |
| MMP3-R | AAGCAGGATCACAGTTGGCTGG |
| MMP9-F | GCCACTACTGTGCCTTTGAGTC |
| MMP9-R | CCCTCAGAGAATCGCCAGTACT |
| ABCC1-F | CCGTGTACTCCAACGCTGACAT |
| ABCC1-R | ATGCTGTGCGTGACCAAGATCC |
| β-Actin-F | CACCATTGGCAATGAGCGGTTC |
| β-Actin-R | AGGTCTTTGCGGATGTCCACGT |

## References


1 J. R. Carreon, M. A. Roberts, L. M. Wittenhagen and S. O. Kelley, *Org. Lett.*, 2005, **7**, 99-102.

2 S. Kim, H. Jo, M. Jeon, M. G. Choi, S. K. Hahn and S. H. Yun, *Chem. Commun.*, 2017, **53**, 4569-4572.

3 D. C. Neckers and J. Paczkowski, *Tetrahedron*, 1986, **42**, 4671-4683.

4 S. Wen, Y. Liu, F. Wang, G. Lin, J. Zhou, B. Shi, Y. D. Suh and D. Jin, *Nat Commun.*, 2020, **11**, 6047.

5 Y. Chen, J. Zhang, X. Liu, S. Wang, J. Tao, Y. Huang, W. Wu, Y. Li, K. Zhou, X. Wei, S. Chen, X. Li, X. Xu, L. Cardon, Z. Qian and M. Gou, *Sci Adv.*, 2020, **6**, eaba7406.